Eur. Phys. J. B **60**, 273–279 (2007)
DOI: 10.1140/epjb/e2007-00349-2

THE EUROPEAN PHYSICAL JOURNAL B

High resolution diffraction and small angle scattering neutron investigations of $LaCo_{0.5}Mn_{0.5}O_{3+\delta}$: effect of oxygen content

D.V. Karpinsky[1,a], I.O. Troyanchuk[1], A.P. Sazonov[1], O.A. Savelieva[2], and A. Heinemann[3]

[1] Institute of Solid State and Semiconductor Physics, National Academy of Sciences, Brovki str. 19, Minsk, 220072 Belarus
[2] M.V. Lomonosov Moscow State University, 119899 Moscow, Russia
[3] Berlin Neutron Scattering Center, Hahn-Meitner-Institute, Glienicker str. 100, 14109 Berlin, Germany

Received 5 February 2007
Published online 22 December 2007 –

Abstract. We have investigated $LaCo_{0.5}Mn_{0.5}O_{3+\delta}$ compounds with different oxygen content by means of magnetization, high resolution and small-angle neutron diffraction measurements. Oxygen content decrease down to stoichiometric composition leads to an essential increase of T_C and magnetic moment while Co/Mn ionic ordering degree is kept almost constant. It is assumed that upon oxygen reduction Co^{3+} ions change their valence state down to 2+ one that leads to dominating of Co^{2+}-Mn^{4+} ferromagnetic interactions as well as T_C increase. Magnetic properties can be explained in terms of coexistence of long-range ferromagnetic order and short-range clusters with antiferromagnetic interactions prevailing. Size distribution of the mentioned short-range magnetic inhomogeneities is rather mild within the samples but it is strongly temperature dependent.

PACS. 75.25.Ha – 74.62.Bf Effects of material synthesis, crystal structure, and chemical composition – 75.25.+z Spin arrangements in magnetically ordered materials

1 Introduction

Solid solutions with chemical formula $LnMn_{1-x}M_xO_3$ (Ln-lanthanide, M-transition metal ions) are of considerable interest because of their peculiar magnetic properties [1–8]. Such materials show promising properties like ferromagnetic ordering near room temperature [5–9], metamagnetic transformations [6–8], etc. Some of them (so-called multiferroics) possess both ferroelectricity and ferromagnetism, e.g. $BiCo_{0.5}Mn_{0.5}O_3$ [10].

An origin of ferromagnetism in the mentioned solid solutions is still controversial. Goodenough interpreted the ferromagnetic interactions in the $LaMn_{0.5}Co_{0.5}O_3$ as a consequence of dynamic Jahn-Teller effect of octahedrally coordinated Mn^{3+} ions that results in positive superexchange interactions Mn^{3+}-O-Mn^{3+} [1]. Another model explaining magnetic properties of the mentioned compound assumes Co^{2+}-Mn^{4+} valence configuration which has been proposed firstly by Blasse [11] based on magnetic susceptibility results. In [5,6,12,13] the magnetic properties explanation for the $LaMn_{0.5}Co_{0.5}O_3$ compound has been based on different degree of Co^{2+}-Mn^{4+} ionic ordering. Proposed model explains anomalies observed in $M(T)$ dependence at 150 and 220 K assuming phase separation: the high temperature maximum in $M(T)$ curve is caused by a phase with well ordered Co^{2+}-Mn^{4+} ions, whereas disordered fraction of Co^{2+}-Mn^{4+} ions results in the low temperature maximum. It is known [14] that preparation conditions determine magnetic properties of the $LaMn_{0.5}Co_{0.5}O_3$ compound. Thus high temperature solid state reaction synthesis favors stabilization of low temperature anomaly (∼150 K) which is caused by positive Co^{2+}-Mn^{4+} ions interactions [15], whereas low temperature preparation methods promote magnetic anomaly near 225 K [15] which is governed by ferromagnetic Mn^{3+}-Mn^{3+} superexchange interactions. Synthesis temperature in the 700–1300 K interval provide compounds containing two mentioned anomalies. By means of XANES technique authors [16] argued that mixed valence states of Co^{2+}/Co^{3+} and Mn^{3+}/Mn^{4+} exist in all solid solutions $LaCo_{1-x}Mn_xO_3$ prepared by high temperature synthesis.

In order to elucidate an origin of magnetic interactions in $LaCo_{1-x}Mn_xO_3$ system a substitution of the Co ions by some other ones has been used as an effective method. Studying Al doped $LaCo_{1-x}Mn_xO_3$ solid solutions authors [17] revealed that Co ions play an essential role in magnetic properties determination so not only Mn^{3+} ions are responsible for ferromagnetism in La_2MnCoO_6.

Recently authors in [18] claimed a spin glass component in nanocrystalline ferromagnet $LaMn_{0.5}Co_{0.5}O_3$. An existence of glassy behavior in a long-range-ordered

[a] e-mail: karpinsky@ifttp.bas-net.by

magnetic material complicates the magnetic properties understanding.

It's well known that crystal and magnetic properties of cobaltites and manganites are strongly dependent on preparation conditions and following thermal treatment in gaseous medium. We present here a high resolution neutron diffraction and a small angle neutron scattering (SANS) investigations as well as magnetization measurements of the $LaMn_{0.5}Co_{0.5}O_{3+\delta}$ compounds ($\delta = -0.03$, 0, 0.05). Combining these data with already available ones [15,19] we have made an attempt to clarify a role of Co/Mn ionic ordering degree as well as their valence and spin state in magnetic properties of $LaMn_{0.5}Co_{0.5}O_{3+d}$ compounds.

2 Experimental

Polycrystalline sample $LaMn_{0.5}Co_{0.5}O_{3+d}$ has been prepared by a conventional solid state reaction technique. The appropriate amounts of La_2O_3, Co_3O_4 and Mn_2O_3 have been ground and then calcined at 1200 K. The sample has been sintered at 1620 K during 6 h (a synthesis has been repeated several times with intermediate grindings). Phase purity control performed on DRON-3M diffractometer with Cu-K_α radiation revealed that sample prepared at first steps has certain tails of the phases close to extreme members – $LaCoO_3$ and $LaMnO_3$. Slowly cooled final sample has been calculated as a single phase. The oxygen content has been determined by calculating the changes in the samples weight after reducing it down to simple oxides. An oxygen content value of 3.05 ($\delta = 0.05$) has been estimated for the as-prepared sample that assumes a presence of cation vacancies predominantly in A-site position [20].

Two parts of the synthesized in air sample have been reduced in evacuated quartz ampoules at 1200 K thus authors got a stoichiometric sample ($\delta = 0$) and that with a little oxygen deficit ($\delta = -0.03$). Tantalum metal has been used as an oxygen getter. Oxygen content for these samples has been determined by the same procedure as in the case for the as-prepared compound. SANS measurements have been done at a wavelength of 6 Å, at $0.005 < q < 0.3$ Å^{-1} range. The data refinement has been performed using the HMI-standard "BerSANS" software package. The high resolution neutron diffraction study has been carried out using the FIREPOD diffractometer ($\lambda = 1.7971$ Å) at the Hahn-Meitner Institute (BENSC, Berlin). The structures have been refined by the full-pattern Rietveld method using the program "FullProf" [21]. Magnetic measurements have been performed using MPMS SQUID (Quantum Design) and VSM magnetometers.

3 Results

Ambient temperature X-ray diffraction studies have confirmed a single-phase structure for all three samples which have been easily indexed in orthorhombic space group (S.G.) Pbnm (#62). The lattice parameters calculated are in good agreement with the already published ones [22].

More detailed crystal structure refinement has been performed using high resolution neutron diffraction measurements. All the samples have been studied at 2 and 300 K. Rietveld analysis of neutron diffraction data have been performed in models assuming single orthorhombic and monoclinic phases. The best reliability factors for NPD spectra have been refined in monoclinic symmetry using $P2_1/n$ S.G. (#14). A symmetry decrease to this space group allowed ones to distinguish between B sites occupied by Co and Mn ions. Lattice parameters, coordinates, significant interatomic distances and angles as obtained from the neutron data are shown in Table 1.

The initial structure parameters have been taken from [23], starting transition metal ions occupations have been set to 0.25:0.25 assuming a total disorder. The sum of the occupancies values for TM ions sites has been limited by 0.5 for each B position (2d and 2c) throughout the refinement, whereas the rest ions' occupation values have been limited in a range of 0.9–1.1 and unlocked at the final stages of the refinement. The estimated oxygen content for all the samples are in agreement with our experimental data.

The best reliability factors for 2 K neutron diffraction patterns have been obtained in the same S.G. ($P2_1/n$) with additionally introduced magnetic phase. The most noticeable peaks which increased at low temperature have been indexed as (110) and (020) – assuming the given S.G. one can ascribe them to ferromagnetic phase. The observed and the calculated profiles as well as the difference curve for the $LaCo_{0.5}Mn_{0.5}O_3$ are given in Figure 1. The maximum magnetic moment of 2.6 μ_B has been estimated for the oxygen stoichiometric compound. Such a value is less than declared for highly ordered compounds [19] and one can suppose an inhomogeneous magnetic structure of the sample. A deviation from stoichiometry leads to essential decrease of magnetic moment value especially in the case of the as-prepared sample (see Tab. 1).

The important data about chemical composition of the samples can be treated from the ions occupation values. An average ratio of B cation occupations about 0.14 : 0.36 is estimated for the oxygen stoichiometric compound at 2 K, this is a maximal ordering value calculated for the samples under study. Such value assumes a certain part of ordered structure. One can easily estimate B cation ordering degree checking the inset of Figure 1, where several ordering ratio are presented. Brief inspection confirms the results of NPD analysis. For the as-prepared sample the transition ions have almost the same ordering degree at 2 K (corresponding B site occupation ratio is 0.18 : 0.32) assuming greater amount of antisite defects. One should notice (Tab. 1) what almost the same ordering degree has been estimated for the oxygen deficit sample. We should note that ordering degree rather weakly depends on oxygen content as one can conclude from Rietveld analysis (Tab. 1) or just comparing shape and intensity of (101)|(011) reflection which is responsible for B cation ordering (Fig. 1 inset). The B cations ordering degree shows

Table 1. The results of crystal and magnetic structure refinement of the NPD data.

Composition	$LaCo_{0.5}Mn_{0.5}O_{2.97}$		$LaCo_{0.5}Mn_{0.5}O_3$		$LaCo_{0.5}Mn_{0.5}O_{3.05}$	
Temperature, K	2	300	2	300	4	300
a, Å	5.51403(11)	5.52479(11)	5.51021(17)	5.52067(18)	5.50837(15)	5.52062(19)
b, Å	5.48336(10)	5.48759(11)	5.47300(16)	5.47829(17)	5.47080(15)	5.47692(18)
c, Å	7.77512(16)	7.78595(18)	7.7649(3)	7.7743(3)	7.74940(20)	7.7614(3)
β, °	89.970(7)	89.983(9)	89.985(10)	89.984(10)	89.964(7)	89.977(9)
V, $Å^3$	235.08(1)	236.05(1)	234.17(1)	235.12(1)	233.53(1)	234.68(1)
$\mu_{Co/Mn}$, μ_B	2.24(6)	-	2.54(7)	-	2.22(10)	-
La:						
x	0.9957(7)	0.9967(7)	0.9969(8)	0.9981(8)	0.9983(7)	0.9975(8)
y	0.0228(4)	0.0205(4)	0.0227(4)	0.0205(5)	0.0234(4)	0.0221(6)
z	0.2521(17)	0.2497(18)	0.2564(11)	0.2551(11)	0.2534(13)	0.252(2)
O(1):						
x	0.0655(7)	0.0655(7)	0.0669(8)	0.0664(8)	0.0668(7)	0.0656(9)
y	0.4899(6)	0.4918(8)	0.4935(6)	0.4949(8)	0.4934(8)	0.4957(11)
z	0.251(3)	0.250(3)	0.2450(20)	0.2435(17)	0.247(2)	0.255(3)
O(2):						
x	0.7314(17)	0.734(2)	0.7322(14)	0.7360(15)	0.7348(16)	0.732(2)
y	0.275(3)	0.266(2)	0.2710(20)	0.2678(18)	0.2878(16)	0.281(2)
z	0.0386(18)	0.0399(13)	0.0349(15)	0.0306(11)	0.0314(12)	0.0294(14)
O(3):						
x	0.7190(19)	0.721(2)	0.7134(15)	0.7155(17)	0.7155(16)	0.720(2)
y	0.276(3)	0.2812(19)	0.2800(20)	0.2822(19)	0.2671(16)	0.265(2)
z	0.4649(18)	0.4679(13)	0.4654(15)	0.4625(12)	0.4609(12)	0.4591(14)
M(1)-O(1), Å	1.97(2)	1.98(2)	2.014(15)	2.028(13)	1.995(15)	1.94(2)
M(1)-O(2), Å	1.998(14)	1.975(11)	1.979(10)	1.978(9)	2.052(9)	2.015(11)
M(1)-O(3), Å	1.996(13)	1.970(11)	2.004(9)	1.994(10)	2.042(9)	2.036(11)
⟨M(1)-O⟩, Å	1.988	1.975	1.999	2.001	2.029	1.997
M(2)-O(1), Å	1.990(2)	1.980(2)	1.938(15)	1.929(13)	1.950(15)	2.010(2)
M(2)-O(2), Å	1.951(13)	1.976(11)	1.955(9)	1.949(9)	1.882(9)	1.918(11)
M(2)-O(3), Å	1.955(15)	1.983(11)	1.950(10)	1.972(10)	1.907(9)	1.919(11)
⟨M(2)-O⟩, Å	1.965	1.980	1.948	1.950	1.913	1.949
M(1)-O(1)-M(2), °	158.8(9)	158.8(9)	158.4(6)	158.6(5)	158.4(6)	158.8(9)
M(1)-O(2)-M(2), °	159.9(5)	160.5(5)	161.9(4)	164.3(4)	161.3(4)	162.6(5)
M(1)-O(3)-M(2), °	159.5(6)	160.0(4)	158.2(4)	157.3(4)	158.8(4)	158.9(5)
R_{Bragg}, %	4.92	6.12	3.73	4.81	5.38	5.86
χ^2, %	1.68	1.63	1.99	2.25	3.08	1.49
R_{Magn}, %	12.6	–	6.36	–	12.5	–
Magn. Moment	2.46(1)	–	2.57(1)		2.22(1)	

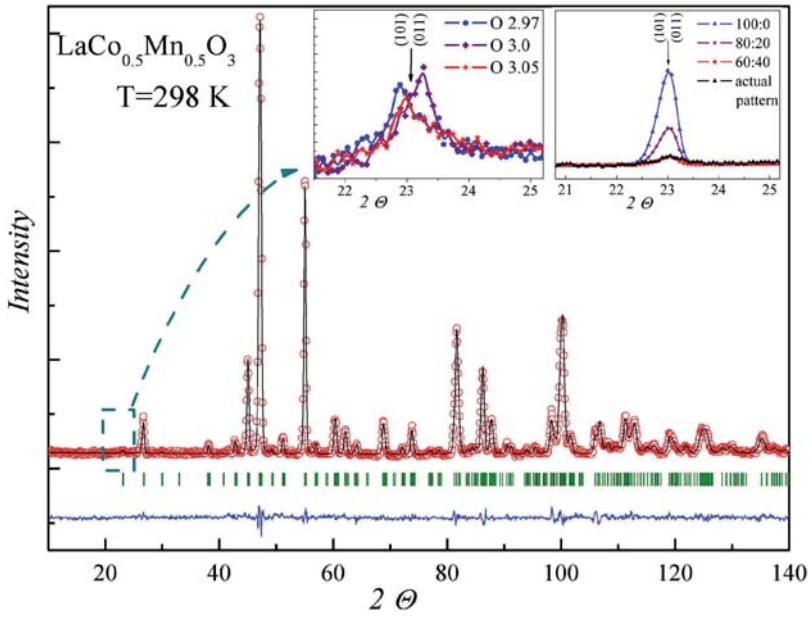

Fig. 1. The refined 298 K NPD pattern for $LaCo_{0.5}Mn_{0.5}O_3$ compound. The observed intensities are shown by dots and the calculated ones by solid line. The positions of the Bragg reflections are shown by the small vertical lines below the patterns. The line at the bottom indicates the intensity difference between the experimental and the refined patterns. The left inset shows the most responsible for B cation ordering peak for all the samples under study at 298 K, the right one indicate intensities of the mentioned peak for several modeled ordering ratio.

hardly noticeable changes with temperature increase, and remains almost the same in wide temperature range [23] assuming steady cation order.

An essential information about ions occupied 2c and 2d positions (S.G. $P2_1/n$) has been derived from an analysis of the (Co/Mn)-O bond lengths. The average (Co/Mn)-O bond lengths of the oxygen stoichiometric sample at 300 K are 2.001 and 1.950 Å for 2d and 2c positions respectively. There no any noticeable changes have been observed for (Co/Mn)-O bond lengths with temperature decrease. Based on the data available [23–25] one can suppose that 2d position is occupied mainly by Co ions in most probably 2+ valence state, whereas 2c one is kept by Mn ions presumably in 4+ electronic state. For the as-prepared compound an average (Co/Mn)-O bond length corresponding 2d position is slightly decreased (1.997 Å) while another one remain almost the same (1.949 Å). Assuming electroneutrality principle and changes, observed in the bond lengths, one can suppose that Co^{3+} ions can locate in both 2c and 2d positions. The corresponding bond lengths for the oxygen deficit sample are almost equal that assumes more complex distribution of B cations.

A type of antisite defects, viz., a valence state and an allocation of the ions occupying "unexpected" positions is essential question and to a greater extent causes magnetic properties of the samples. Possible scenario explaining magnetic properties of the samples based on valence ions state and their distribution is described in the discussion section.

The temperature dependences of magnetization have been measured in a magnetic field of 100 Oe in the field cooled (FC) and zero field cooled (ZFC) modes. One can easily estimate the onset of magnetic transition, it is about 160 K for the as-prepared sample, what is essentially less than for the rest samples (∼215–220 K). All the $M(T)$ curves are typically ferromagnetic for all the samples (Fig. 2). Despite certain similarity of the FC curves trends of the stoichiometric and the oxygen deficit samples, some little discrepancies still exist (e.g. slight deviation in transition temperatures and more gradual FC curve decrease for the reduced sample), pointing toward some distinctions in magnetic interactions within the samples. For all the samples a large deviation between FC and ZFC curves immediately after a transition temperature has been observed. It assumes an essential magnetic anisotropy of the materials. In [26] such magnetization behavior has been explained by existence of weak interacting magnetic clusters within the sample. Based on these data we can not draw a conclusion that such clusters do exist. At least there are no distinct magnetic anomalies peculiar for cluster glass observed on $M(T)$ curves.

There is no saturation observed in the field dependence curves even at rather high magnetic fields. The $M(H)$ magnetization revealed a noticeably lower magnetic moment for the as-prepared sample than that claimed in [27] where spin only magnetic moments was claimed to be 4 μ_B for Co^{3+}-Mn^{3+} valence configuration and 3.88 μ_B for Co^{2+}-Mn^{4+} one, but magnetic moment values we got from isothermal magnetization curves are in accordance with the data obtained from neutron data analysis (see

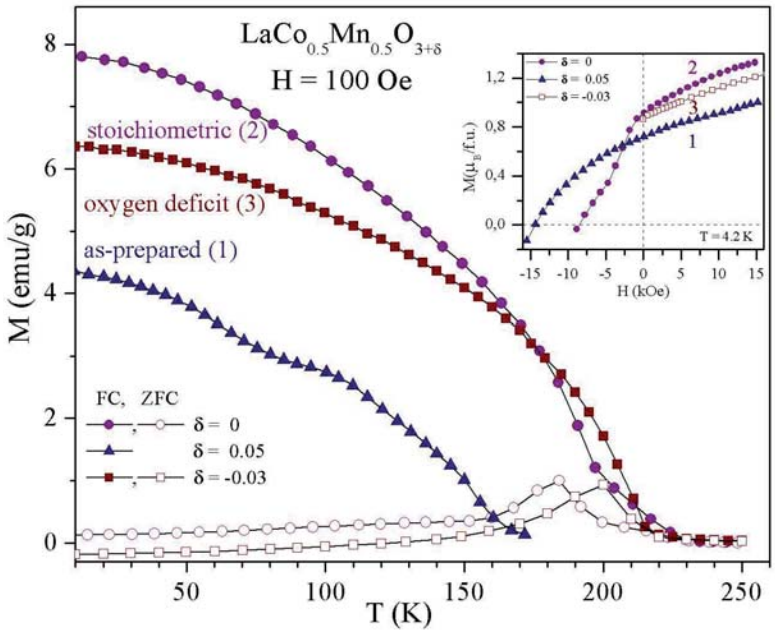

Fig. 2. Temperature dependences of the magnetization as measured in the FC and ZFC (except the as-prepared sample) modes for the samples under study. The inset shows field dependences of the samples.

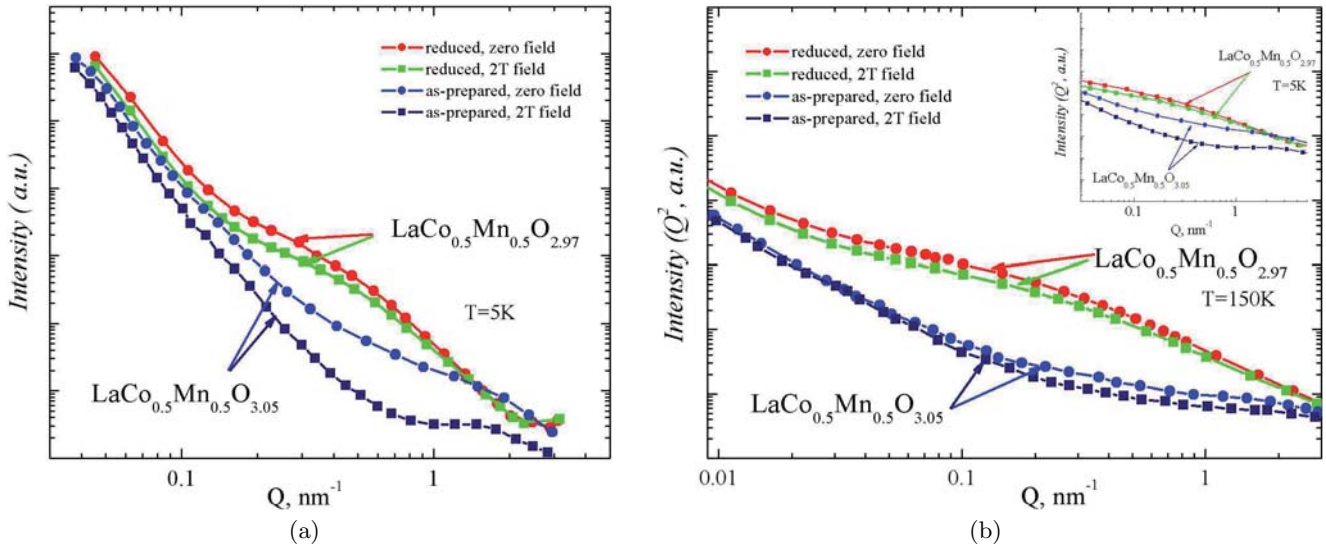

Fig. 3. Q (a) and Q^2 (b) dependences of the SANS intensity for the oxygen deficit and the as-prepared compounds.

below). Possibly certain magnetic inhomogeneity can be assumed from the data obtained but its origin is still ambiguous. More clear information about an intrinsic magnetic and crystal structure of the samples can be derived from the SANS data given below.

The SANS patterns for the $LaMn_{0.5}Co_{0.5}O_{3.05}$ and the $LaMn_{0.5}Co_{0.5}O_{2.97}$ samples have been measured in 5–250 K temperature range. The scattering curves have been measured at different temperatures, the more informative of them are shown in Figure 3. It is clear that patterns can be separated in two regions depending on intensity-low q (due to long-range scattering) and higher q (short-range one). To estimate size distribution of scattering regions we have used radius of gyration as a universal characteristic parameter. The $I(q)$ curves have been drawn like $\mathrm{Ln}(q) = f(q^2)$ and linear parts of the obtained curves have been analyzed (see Fig. 3b).

At constant temperature a deviation of a $f(q^2)$ curve from linear is insignificant thus pointing that distribution of particles size to be rather mild and this is valid for both the samples in a temperature range considered. At low temperatures maximum contribution to the neutron scattering is from the particles about a hundreds angstrom. Spherical shape particles should give a Q^{-4} variation what is really seen for both the samples for low Q region (Fig. 3a). For the oxygen deficit compound a Q^{-2} contribution has an essential contribution in the 0.2–0.6 nm^{-1} Q interval what is characteristic for 2 D layered structure [28]. Neutron scattering for the as-prepared

sample consists from components with different Q exponent assuming more complex clusters shape.

In order to separate magnetic scattering contribution from nuclear one the samples have been located in homogeneous magnetic field perpendicular to primary neutron beam direction. The magnetic flux density has been turned up to $2T$ ($4T$ for the reduced sample) when magnetic moments of the compounds are nearly aligned.

A magnetic field application cause neutron scattering reduction (Fig. 3), a possible scenario of such behavior is mentioned in discussion section. We have plot scattering curves recorded with and without magnetic field, so, one can estimate the particles with the most sensitive size to the magnetic field given. A difference between scattering curves recorded with and without magnetic field became almost negligible near a magnetic transition temperature what is in accordance with magnetization measurements results, whereas at liquid helium temperature the mentioned curves deviate in a whole q region measured. Such sensibility to magnetic field application observed at low q region points towards long-range magnetic ordering. We should note that such a deviation persist up only to 100 K for the as-prepared sample and just below 20 K for the oxygen deficit one.

4 Discussion

It has been revealed that crystal structure for all the samples can be well described assuming $P2_1/n$ S.G. in a rather wide temperature range (up to 300 K). A supposed ionic order persists up to high temperatures (about 600 K [23]) then crystal structure is characterized by rhombohedral distortions ($R\bar{3}$S.G.). We should note that certain ionic ordering is kept despite some changes of elements content within the compounds.

But even in the stoichiometric sample, where the B cation ordering degree is most pronounced, essential amount of antisite defects are present (Tab. 1). Based on the data available one can not draw a conclusion about localized character of the ordered fraction of the compounds. Most probably it is strongly bound with a host ferromagnetic matrix and caused by different local surroundings of the Co/Mn ions assuming all sets of the coordinations. Depending on Co/Mn ions ratio and valence state such formations can show either paramagnetic or antiferromagnetic behavior.

Based on the estimated bonds lengths and ordering degree one can draw a supposition that in the stoichiometric compound the antisite ions mainly have the same valence state like "original" ones and in spite of disadvantages in elastic energy, there are only small part of antisite ions in 3+ valence state. A charge state of the ions for the non-stoichiometric compounds became more complex because of changes of elements content within the compounds.

Taking into account changes in the (Co/Mn)-O bond lengths and the obtained B site occupation ratio for the as-prepared sample in comparison with the stoichiometric one, we can draw a conclusion that the Co^{3+} ions are allocated in 2c and 2d positions. In spite of cation vacancies, mixed valence and charge state of the transition metal ions, certain ionic order persists in a temperature range measured. Most likely that the as-prepared compound contains about 20% of Co^{3+} ions in the low spin state which frustrate positive magnetic interactions between Co^{2+}-Mn^{4+} ions thus causing an essential decrease of total magnetization. An oxygen content decrease lead to reduction of 3+ valence state of Co ions down to 2+ one resulting to essential increase of positive Co^{2+}-Mn^{4+} interactions and consequently magnetization value.

Further oxygen content decrease lead to oxygen vacancies occurring, which are in most cases situated within the mentioned clusters and frustrate magnetic interactions and one can see an only slightly decreased spontaneous magnetization of the reduced sample in comparison with the oxygen stoichiometric one.

Discussing the above-mentioned properties we have deviated slightly from the structure of the samples. Let's have a look at a micro level of the samples addressing to the SANS data.

We have estimated that scattering regions for both of the studied samples have nearly spherical shape for low Q region and form host matrix whereas for higher Q they have rather complex shape for the as-prepared sample and resemble 2 D formations for the oxygen deficit compound. Clusters with such a small size (Q range more than 0.2 nm^{-1}) are strongly temperature dependent. Most probably that at low temperature coalescence of the clusters begins. But for the as-prepared sample one can observe their percolation about 100 K whereas for the oxygen deficit sample coalescence occurs below 20 K only. These clusters start melting with temperature increase and have less than hundred angstrom size near the magnetic transition temperature. At high temperatures the interactions between such formations are almost neglible.

From the analysis of valence and spin state of antisite defects and taking into account magnetization measurements one can suppose that mentioned clusters most probably have AF nature.

That for the oxygen deficit sample clusters coalescence occurs at such a low temperature can be explained by scenario, according to which anion vacancies frustrate Co/Mn interatomic interactions and decrease clusters size. As A-cation vacancies in the as-prepared sample do not participate actively in magnetic interactions and AF clusters keep they structure formed by synthesis process.

Scattering intensity decreases with magnetic field applying can be explained by magnetic moments alignment within the clusters at strong magnetic field. Thus an angle between magnetic moments and scattering vectors decreases what leads to reduction of magnetic interactions between incident neutron flux and magnetic ions.

Taken two characteristic cluster sizes (Fig. 4) we have evaluated a dynamic of clusters size changing with temperature. One can notice an absence of any abrupt increase in neutron scattering caused by magnetic interactions, unlike $La_{1-x}Sr_xCoO_3$ compounds where such feature has been observed above percolation boundary ($x > 0.2$) [29]. An absence of the neutron scattering increase near the magnetic transition temperature assumes that the mentioned

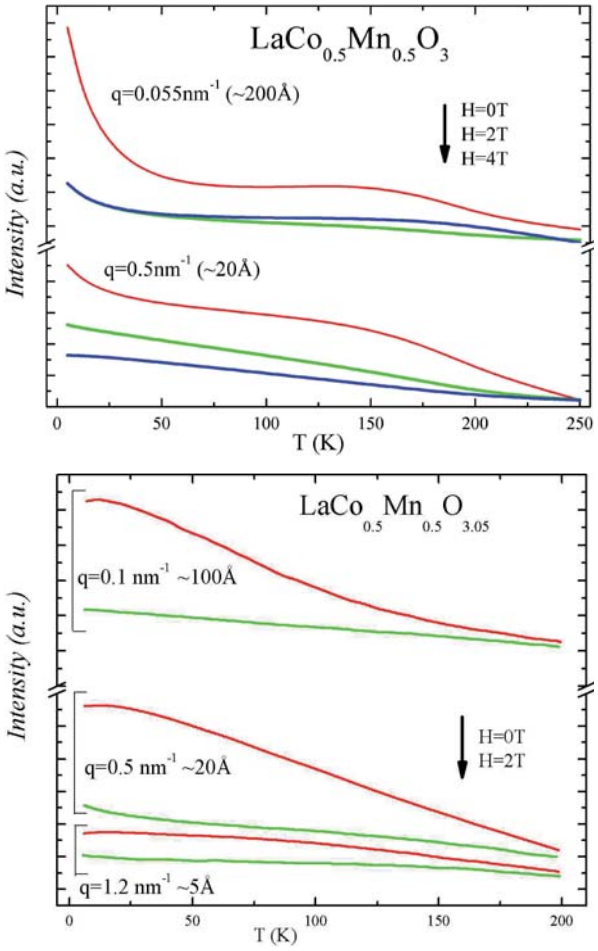

Fig. 4. The scattering intensities of the selected size clusters measured with and without magnetic field applying.

clusters are not separated from the rest matrix and keep certain binding with it.

5 Conclusion

The investigations performed incline authors that magnetic structure of the samples assumes spin-glass component within the samples. Parallel with long range magnetic ordering which is undoubtedly exists as seen from magnetization and high resolution neutron study a small spin-glass component plays a certain role in magnetic properties of the samples. The most probable scenario explaining magnetic properties of the compounds assumes a coexistence of long-range ferromagnetic matrix with Co^{2+}-Mn^{4+} dominated interactions and clusters with short range antiferromagnetic coupling. Most probably the key role in magnetic properties determination plays a valence state of transition metal ions rather than their ordering degree. This provides an indication of intricate behavior of the magnetic materials under study what asserts a further interest of them to a scientific community.

The work was supported partly by European Commission under the 6th Framework Programme through the Key Action: Strengthening the European Research Area, Research Infrastructures; Contract no. RII3-CT-2003-505925 (NMI3), RFBR 06-02-8102.

References

1. J.B. Goodenough, A. Wold, R.J. Arnott, Phys. Rev. **124**, 373 (1961)
2. G.H. Jonker, J. Appl. Phys. **37**, 1425 (1966)
3. J.-H. Park, S.-W. Cheong, C.T. Chen, Phys. Rev. B **55**, 17, 11072 (1997)
4. J. van Elp, Phys. Rev. B **60**, 7649 (1999)
5. R.I. Dass, J.B. Goodenough, Phys. Rev. B **67**, 014401 (2003)
6. I.O. Troyanchuk, L.S. Lobanovsky, D.D. Khalyavin, S.N. Pastushonok, H. Szymczak, J. Magn. Magn. Mater. **210**, 63 (2000)
7. I.O. Troyanchuk, D.D. Khalyavin, J.W. Lynn, J. Appl. Phys. **88**, 1, 380 (2000)
8. I.O. Troyanchuk, N.V. Samsonenko, A. Nabialek, H. Szymczak, J. Magn. Magn. Mater. **168**, 309 (1997)
9. R. Mahendiran, Y. Breard, M. Hervieu, B. Raveau, P. Schiffer, Phys. Rev. B **68**, 104402 (2003)
10. M. Azuma, K. Takata, T. Saito, S. Ishiwata, Y. Shimakawa, M. Takano, J. Am. Chem. Soc. **127**, 8889 (2005)
11. G. Blasse, J. Phys. Chem. Solids **26**, 1969 (1965)
12. I.O. Troyanchuk, L.S. Lobanovsky, D.D. Khalyavin, S.N. Pastushonok, H. Szymczak, J. Magn. Magn. Mater. **210**, 63 (2000)
13. I.O. Troyanchuk, A.P. Sazonov, H. Szymczak, D.M. Tobbens, H. Gamari-Seale, JETP **126**, 1 (2006)
14. V.L. Joseph Joly, Y.B. Khollam, P.A. Joy, C.S. Gopinath, S.K. Date, J. Phys.: Condens. Matter **13**, 11001 (2001)
15. V.L. Joseph Joly, P.A. Joy, S.K. Date, C.S. Gopinath, J. Phys.: Condens. Matter **13**, 649 (2001)
16. M. Sikora, Cz. Kapusta, K. Knížek, Z. Jirák, C. Autret, M. Borowiec, C. J. Oates, V. Procházka, D. Rybicki, D. Zajac, Phys. Rev. B **73**, 094426 (2006)
17. V.L.J. Joly, P.A. Joy, Solid State Comm. **130**, 691 (2004)
18. R. Mahendiran, Y. Breard, M. Hervieu, B. Raveau, P. Schiffer, Phys. Rev. B **68**, 104402 (2003)
19. R.I. Dass, J.B. Goodenough, Phys. Rev. B **67**, 014401 (2003)
20. R.I. Dass, J.-Q. Yan, J.B. Goodenough, Phys. Rev. B **68**, 064415 (2003)
21. J. Rodriguez-Carvajal, Physica B **192**, 55 (1993)
22. C. Autret, J. Hejtmanek, K. Knizek, M. Marysko, Z. Jirak, M. Dlouha, S. Vratislav, J. Phys.: Condens. Matter **17**, 1601 (2005)
23. C.L. Bull, D. Gleeson, K.S. Knight, J. Phys.: Condens. Matter **15**, 4927 (2003)
24. J.-Q. Yan, J.-S. Zhou, J.B. Goodenough, Phys. Rev. B **69**, 134409 (2004)
25. P.G. Radaelli, M. Marezio, H.Y. Hwang, S.-W. Cheong, B. Batlogg, Phys. Rev. B **54**, 8992 (1996)
26. H. Cheng, L.-S. Wang. Phys. Rev. Lett. **77**, 51 (1996)
27. P.A. Joy, Y.B. Khollam, S.K. Date, Phys. Rev. B **62**, 8608 (2000)
28. D. Saurel, S. Mercone, N. Guiblin, V. Hardy, A. Brulet, C. Martin, Ch. Simon Physica B **350**, 51 (2004)
29. Wu, J.W. Lynn, C.J. Glinka, J. Burley, H. Zheng, J.F. Mitchell, C. Leighton, Phys. Rev. Lett. **94**, 037201 (2005)